Evaluation of fracture toughness of small volumes by means of cube-corner nanoindentation

N. Cuadrado,[a,*] D. Casellas,[a,b] M. Anglada[c] and E. Jiménez-Piqué[c]

[a]*Fundació CTM Centre Tecnològic, Avda. de les Bases de Manresa 1, 08242 Manresa, Spain*
[b]*Department of Materials Science and Metallurgical Engineering, EPSEM, Universitat Politècnica de Catalunya, Avda. de les Bases de Manresa 61, 08242 Manresa, Spain*
[c]*Department of Materials Science and Metallurgical Engineering, ETSEIB, Universitat Politècnica de Catalunya, Avda. Diagonal 647, 08028 Barcelona, Spain*

In this work, the applicability of the two most commonly used equations for calculating the fracture toughness by nanoindentation is discussed in terms of indenter geometry and indentation crack morphology. These equations are calibrated for Berkovich and cube-corner indenters taking into account the actual indentation crack morphology, in order to attain a more reliable estimation of fracture toughness in small material volumes by nanoindentation.
© 2012 Acta Materialia Inc. Published by Elsevier Ltd. All rights reserved.

Mechanical characterization of micro-volume systems such as thin films [1,2] or micro-sized phases [3] is a critical step for optimizing and developing materials and high-performance coatings. Nanoindentation has proved to be a suitable technique for the mechanical characterization of micro-sized material volumes in terms of hardness (H), Young's modulus (E) and fracture toughness in mode I (K_{Ic}). While H and E are measured from load–displacement curves [4], K_{IC} is estimated from the length of indentation cracks following the indentation microfracture method (IM). It is based on the formation of cracks at the indentation corners when sharp indenters are applied. Such indentation cracks extend, driven by the residual stress field up to a length that can be related to the material crack propagation resistance. The use of indentation as a technique for measuring fracture toughness was proposed in the 1970s by Evans and Charles who related the stress intensity factor (K) for Vickers indentation cracks to the observed crack lengths [5]. Since then, many expressions to compute K_{IC} by indentation have been proposed [6]. Two of the most used are the equations proposed by Anstis et al. [7] and by Laugier [8]. Both equations are based in the Lawn et al. extension of the Evans and Charles analysis [5]. Lawn et al., by using Hill's expanding cavity solution for an elastic-plastic solid and assuming a half-penny crack configuration, suggested the following expression to calculate K_{IC} [5]:

$$K_{IC} = \xi_R \left(\frac{E}{H}\right)^{1/2} \frac{P}{c^{3/2}} \qquad (1)$$

where E is the Young's modulus, H is the hardness, P is the indentation load and $2c$ is the total crack length (i.e. $2c = 2l + 2a$, where l is the length of the crack from the indentation corner, and $2a$ is the indentation diagonal). The term ξ_R is a material constant containing elements related to the geometry of the indenter and the morphology of the crack system (taken to be a half-penny). In 1981, Anstis et al. fitted Eq. (1) by using a number of brittle materials with a well-known K_{IC}, ranging from 0.74 MPa m$^{1/2}$ (soda lime glass) to 12 MPa m$^{1/2}$ (cemented WC–Co) [7]. Using the experimental values of E, H, K_{IC} and $P/c^{3/2}$ for each material, the value of ξ_R was found to be 0.016. This value is well established when half-penny cracks are generated with Vickers indenters in the range of macro- and microindentation. On the other hand, for superficial cracks, such as Palmqvist crack profiles, in 1987 Laugier adapted the Lawn half-penny formalism and modified K to take into account the actual crack morphology [8]:

$$K_{IC} = \chi_v \left(\frac{l}{a}\right)^{-1/2} \left(\frac{E}{H}\right)^{2/3} \frac{P}{c^{3/2}} \tag{2}$$

The symbols E, H, P, a and l have the same meaning as in Eq. (1). The fit of the equation for radial cracks leads to a value for the constant χ_v of 0.015 [8]. In spite of serious criticisms to the IM method for the determination of fracture toughness [9], it is still widely used as a simple, rapid and inexpensive method. However, it is well known that if the constants ξ_R and χ_v are not properly calibrated, the accuracy of the obtained values of K_{IC} is low. Such constants were experimentally fitted by Anstis et al. and Laugier, respectively, using four-sided Vickers pyramidal indenters (in the range of macro- and microindentation with applied loads up to 100 N and up to 1000 N in the case of cemented WC–Co) and these are now well accepted and widely used. For three-sided indenters, like Berkovich indenters, less information is available in this high-indentation load range. In 1992, Dukino et al. fitted the Laugier equation (Eq. (2)) by including a modifying factor that accounts for the number of symmetric cracks proposed by Ouchterlony due to the nonsymmetrical nature of Berkovich indenters, obtaining $\chi_v = 0.016$ [10].

Mechanical characterization of small volumes, such as thin films or micro-sized phases, has recently received much attention, and many works have focused on the determination of K_{IC} by nanoindentation following the IM method [3,11–16]. Nanoindentation allows use of the low loads needed for accurate micromechanical characterization with high spatial resolution. However, the first point to consider when extending the applicability of IM to the nanoindentation load range is that the indenters used most frequently for this technique are Berkovich and cube-corner rather than Vickers. Consequently, the fitted ξ_R and χ_v parameters for Vickers indenters must be revised when Berkovich and cube-corner indenters are used since their dependence on indenter geometry and crack morphology should change the fitted values given by Vickers indenters.

Sharper indenters than Berkovich or Vickers indenters, such as the cube-corner indenter, displace a much larger volume of material for a given load. Therefore, higher stresses are induced beneath the indenter, and thus cracks can be generated at lower loads [12]. These sharper indenters allow even smaller material volumes to be characterized [12,13,17]. The morphology of the indentation cracks depends on the indentation load, tip geometry and material toughness. The half-penny morphology, in which cracks are connected underneath the hardness impression, is the most common when testing brittle materials with Vickers indenters and with c/a larger than 3, while radial cracks are developed at low indentation loads or/and in materials with higher toughness, independently of the type of indenter, and with c/a smaller than 2.5 [18].

Accurate K_{IC} measurements require a proper knowledge of the crack morphology in order to select the most appropriate expression for evaluating K_{IC}. From a phenomenological point of view Eq. (1) was developed to be used when half-penny cracks are generated, whereas Eq. (2) was adapted to describe Palmqvist cracks. Despite the number of works addressing the evaluation of fracture toughness by nanoindentation, few deal with the

accuracy of the different expressions for cube-corner indenters [14]. Moreover, K_{IC} is often evaluated by nanoindentation using Eqs. (1), (2), among others, without considering the crack morphology and the indenter tip used. Thus, the aim of the present work is to assess the applicability of the IM method for obtaining K_{IC} of small material volumes by means of nanoindentation, taking into account the influence of the indenter geometry and the generated crack morphology. The constants ξ_R and χ_v of Eqs. (1) and (2) will be fitted by testing materials with well-known K_{IC}.

The materials used in this work have well-known and accepted values of K_{IC}, obtained by standardized procedures, such as the single-edge precracked beam (SEPB), chevron-notched beam (CNB) or surface crack in flexure (SCF) methods, which do not precise experimental calibrations. The fracture toughness of the selected materials must not depend on the crack size, i.e. materials should not present an R-curve behavior. As cracks lengths generated by nanoindentation range from 1 to 9 μm in single crystals, and up to 30 μm in soda lime glass, if an R-curve behavior is present, the toughness developed with such cracks will differ from that obtained from large cracks and calibration using standardized methods will not give accurate results. Accordingly, the following three materials have been chosen: (a) soda-lime glass; (b) Si(100) single crystal; and (c) SiC-6H(0001) single crystal. Table 1 shows the reported K_{IC} values obtained by the SENB method for these materials. In order to obtain more data for the experimental calibration of χ_v for a cube-corner tip geometry, two additional single crystals were analyzed, Si(111) and SiO$_2$(0001). To our knowledge K_{IC} obtained with standardized tests are not available for these two single crystals. To overcome this lack of knowledge K_{IC} was determined by IM using Eq. (2) with $\chi_v = 0.022$ (this value was obtained after calibration with soda-lime glass, Si(100) and SiC-6H(0001) for the Berkovich indenter, see Table 2).

Berkovich and cube-corner indenters were used in a XP Nanoindenter (MTS Corp.) with applied loads in the range of 200 mN–3 N. After indentation, all the hardness impressions and crack morphologies generated were imaged by field-emission scanning electron microscopy (FE-SEM) (Carl Zeiss SMT Inc.) to measure the sizes of the contact impression and the lengths of the cracks emerging from their corners. Crack morphology was examined by means of focus ion beam (FIB) SEM (Carl Zeiss Neon 40). An ion beam of 200 pA and 30 kV was used; SEM images were taken every two ion beam polishing steps and reconstructed using Avizo software. H and E were evaluated using the Oliver–Pharr methodology [4] for performing Berkovich indentation tests, as both are essentially independent of the indenter used [11].
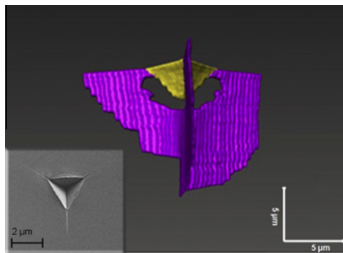
The indented materials showed a well-defined crack pattern in the range of applied loads. Only indentations showing well-developed cracks and without chipping were used to calculate K_{IC}. Figure 1 shows a FIB tomography corresponding to a 100 mN cube-corner indentation on a soda-lime glass sample, where three cracks emanating from the centre of the impression can be observed. Additionally, depending on the indentation

Table 1. K_{IC} comparison using Anstis et al.'s equation and Laugier's equation with the different calibrations of ξ_R and χ_υ reported in Table 2.

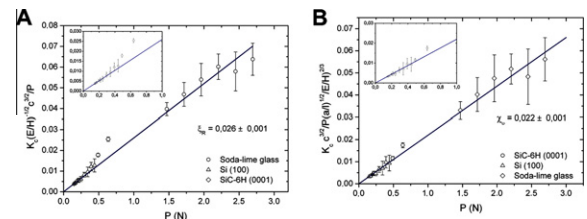| Material	K_{Ic} (MPa m$^{1/2}$)			
	SENB	Berkovich Anstis et al.	Berkovich Laugier	Cube-corner Laugier
SiC-6H(0001)	3.4 [22]	2.3 ± 0.1	3.0 ± 0.3	3.5 ± 0.8
Si(100)	0.95 [23]	0.9 ± 0.2	1.0 ± 0.3	1.0 ± 0.1
Soda-lime glass	0.7 [7]	0.6 ± 0.1	0.6 ± 0.2	0.8 ± 0.1
SiO₂(0001)			1.1 ± 0.1	1.0 ± 0.1
Si(111)			1.4 ± 0.3	1.8 ± 0.2

Table 2. Experimental calibration of the constants ξ_R and χ_υ for a Berkovich and cube-corner indenters for Anstis et al.'s equation (Eq. (1)) and Laugier's equation (Eq. (2)).

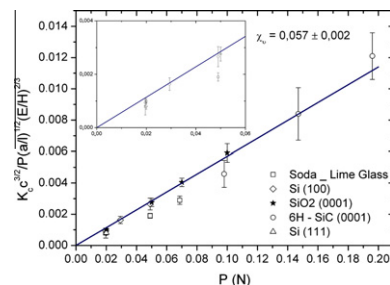| Indenter geometry	Crack morphology	Equation	
		Anstis et al.	Laugier
Vickers	Half-penny	$\xi_R = 0.016$	
Vickers	Radial (Palmqvist)		$\chi_\upsilon = 0.015$
Berkovich	Radial (Palmqvist)	$\xi_R = 0.026 \pm 0.001$	$\chi_\upsilon = 0.022 \pm 0.001$
Cube-corner	Radial (Palmqvist)		$\chi_\upsilon = 0.057 \pm 0.002$

Figure 1. FIB tomography for a cube-corner indenter at 100 mN in a soda-lime glass sample. Radial cracks of semi-elliptical shape can be discerned. Yellow area corresponds to the indentation impression, violet indicates the crack morphology. (For interpretation of the references to colour in this figure legend, the reader is referred to the web version of this article.)

Figure 2. Calibration of the constants ξ_R and χ_υ for a Berkovich indenter in (A) Anstis et al.'s equation (Eq. (1)) and (B) Laugier's equation (Eq. (2)).

load and the tip geometry, lateral cracks were also present. Tomography observations indicate that cracks generated by Berkovich and cube-corner indenters in the three materials evaluated are radial, with a semi-elliptical shape. Accordingly, from a geometric point of view they are not semi-circular and there is no joint between them passing beneath the indentation impression as usually happens under high indentation loads with Vickers indenters. Nevertheless, both constants, ξ_R and χ_υ, from Eqs. (1) and (2), respectively, were determined for the Berkovich indenter, by fitting such equations to the experimental values of H and E, P, the reported value of K_{IC} for each material (Table 1), and the mean crack length (see Fig. 2). The constant ξ_R from Eq. (1) was determined even though this equation was not developed for radial cracks.

The values of ξ_R and χ_υ for Berkovich and cube-corner indenter geometries were experimentally fitted as $\xi_R = 0.026$ and $\chi_\upsilon = 0.022$ or 0.057 depending on the indenter geometry (Table 2). Eq. (2) presents the best fit for Berkovich indenters (Fig. 2). According to this, and because cube-corner indenters produce radial cracks, Eq. (2) was only use to fit the experimental data obtained

with the cube-corner tip (Fig. 3), giving rise to good results. The calculated values of K_{IC} (using the proposed χ_υ for both types of indenters are close to the accepted K_{IC} values for the tested materials (obtained by the SENB method (Table 1)). This good fitting can be rationalized considering the morphology of the indentation crack. Eq. (2) was developed for semi-elliptical radial cracks, the same shape as the experimentally identified cube-corner cracks (which are also semi-elliptical in shape, Fig. 1). The effect of the proper selection of the equation to calculate K_{IC} is shown when calculating fracture toughness with cube-corner indenters. Eq. (2) with $\chi_\upsilon = 0.015$ (obtained by Laugier for a Vickers indenter)

Figure 3. Calibration of the constant χ_υ for a cube-corner indenter in Laugier's equation (Eq. (2)).

gives a K_{IC} for Si(100) of 0.31 ± 0.04 MPa m$^{1/2}$ (calculated in Ref. [13]). However, if the calibrated χ_v for the cube-corner indenter is used ($\chi_v = 0.057$), K_{IC} is 1.0 ± 0.1, which is much closer to the accepted K_{IC} for this material (see Table 2). Thus, it is clear that a proper calibration of experimental equations is crucial to obtain accurate values of K_{IC} by nanoindentation when using Berkovich and cube-corner indenters.

The obtained calibration for cube-corner indenters differs from that obtained in previous works [10,11,13, 15,19,20]. A range of values from 0.033 to 0.040 are reported for cube-corner indenters [11,13,15,19,20], whereas in this work a value of 0.057 has been obtained. If it is assumed that the parameter is related only to tip angle, a value of 0.033 can be expected. On the other hand, depending on the toughness range of the materials studied, a value of 0.0319 [19], 0.036 [11] or 0.040 [20] is reported. The main reason for the discrepancy observed between the literature values and the values given in this work is the equation chosen to fit the experimental data. In the literature, for cube-corner indenters, Eq. (1) was fitted. However, in this work it is shown that the crack morphology has a semi-elliptical shape, which indicates that from a phenomenological point of view Eq. (2) should be used to fit the results. With respect to Berkovich indenters, Dukino et al. reported $\chi_v = 0.016$ (fit performed in the microindentation range, up to 5 N), whereas the value obtained here is slightly different, 0.022 [10]. Such discrepancy could arise from the different formulation of the equations used as discussed above.

Concerning the range of applicability of the proposed values for ξ_R and χ_v, this will be within the fracture toughness values studied, i.e. at least up to 3.4 MPa m$^{1/2}$ This range covers a wide range of glasses and traditional and engineering ceramics.

The experimental calibration of ξ_R and χ_v in this work has been performed using a soda-lime glass and some single crystals. Referring to the latter, crystal anisotropy must be considered when indenting single crystals, since it is known that indentation cracking depends on the crystallographic orientation. In this sense, fracture toughness measurement may be specially sensitive to the relative crystallographic plane–indenter tip orientation. Ebrahimi and Kalwani studied the fracture anisotropy of Si single crystal with Vickers tips, indenting different crystallographic planes and considering the fracture along different crystallographic directions [21]. They show a clear influence of the crystal anisotropy on the fracture toughness. However, K_{IC} remains almost constant when indenting the (001) and (111) planes, but large scatter is found when indenting the (110) plane [21]. Thus, in order to minimize the effect of crystal anisotropy on indentation cracking and to obtain reliable values of ξ_R and χ_v, Si(100) and Si(111) single crystals were chosen to calibrate Eqs. (1) and (2). Experimental assessment involved revising the crack pattern in the tested single crystals, and no evidence was found of preferred fracture directions or abrupt changes in the crack propagation direction for different crystal–tip orientations. Additionally, crack lengths do not vary

significantly; at least the variations are similar to those measured in the amorphous and isotropic sample (soda-lime glass). Such results show that crystal anisotropy does not significantly affect the values of ξ_R and χ_v reported in this work. Nevertheless, crystal anisotropy must be kept in mind when characterizing single crystals by nanoindentation, and accurate analysis of crack patterns is highly recommended, as is consideration of the relative orientation of the indenter tip in the indented plane.

In summary, examination of the crack morphology shows that indentation cracks are radial with a semi-elliptical shape when Berkovich and cube-corner indenters are used in nanoindentation. Therefore, from a phenomenological point of view Laugier's equation would be more suitable for evaluating K_{IC}. Calibration of this equation gives a calibration constant χ_v of 0.022 ± 0.001 for a Berkovich indenter and 0.057 ± 0.002 for a cube-corner indenter, resulting in a nanoindentation fracture toughness close to the actual fracture toughness measured by standardized methods in materials without R-curve behavior.

[1] J. Chen, S.J. Bull, J. Phys. D.: Appl. Phys. 40 (2007) 5401.
[2] J. Malzbender, J.M.J. den Toonder, A.R. Balenende, G. de With, Mat. Sci. Eng. R 36 (2002) 47.
[3] D. Casellas, J. Caro, S. Molas, J.M. Prado, I. Valls, Acta Mater. 55 (2007) 4277.
[4] W.C. Oliver, G.M. Pharr, J. Mater. Res. 7 (1992) 1564.
[5] B.R. Lawn, A.G. Evans, D.B. Marshall, J. Am. Ceram. Soc. 63 (1980) 574.
[6] C.B. Ponton, R.D. Rawlings, Mater. Sci. Technol. 5 (1989) 865.
[7] G.R. Anstis, P. Chantikul, B.R. Lawn, D.B. Marshall, J. Am. Ceram. Soc. 64 (1981) 533.
[8] M.T. Laugier, J. Mater. Sci. Lett. 73 (1987) 897.
[9] G.D. Quinn, R.C. Bradt, J. Am. Ceram. Soc. 90 (3) (2007) 673–680.
[10] R.D. Dukino, M.V. Swain, J. Am. Ceram. Soc. 75 (1992) 3299.
[11] D.S. Harding, W.C. Oliver, G.M. Pharr, Mat. Res. Soc. Symp. Proc. 356 (1995) 663.
[12] J. Jang, G.M. Pharr, Acta Mater. 56 (2008) 4458.
[13] D.J. Morris, R.F. Cook, J. Am. Ceram. Soc. 87 (2004) 1494.
[14] K.I. Schiffmann, Philos. Mag. 91 (2011) 1163.
[15] S.J. Bull, Comp. Rend. Mec. 339 (2011) 5178.
[16] J.M. Jungk, B.L. Boyce, T.E. Buchheit, T.A. Friedmann, Acta Mater. 54 (2006) 4043.
[17] T. Zhang, Y. Feng, R. Yang, P. Jiang, Scripta Mater. 62 (2010) 199.
[18] G.A. Schneider, T. Fett, J. Ceram. Soc. Jpn, 114 (11) (2006), 1044–48.
[19] G.M. Pharr, D.S. Harding, W.C. Oliver, Mechanical Properties and Deformation Behavior of Materials Having Ultra-Fine Microstructures, Dordrecht, Kluwer, 1993, 449.
[20] G.M. Pharr, Mater. Sci. Eng. A-Struct. Mater. Prop. Microstruct. Process. 253 (1998) 151.
[21] F. Ebrahimi, L. Kalwani, Mat. Sci. Eng. A268 (1999) 116.
[22] J.L. Henshall, C.A. Brookes, J. Mat. Lett. 4 (1985) 783.
[23] Y.B. Xin, K.J. Hsia, D.A. Lange, J. Am. Ceram. Soc. 78 (1995) 3201.